Analysis and optimization on single-zone binary flat-top beam shaper

Jame J. Yang
New Span Opto-Technology Incorporated
Miami, Florida

Michael R. Wang, MEMBER SPIE
University of Miami
Department of Electrical and Computer Engineering
Coral Gables, Florida 33124
E-mail: mwang@miami.edu

Abstract. We report on the analysis and optimization of a binary phase element for shaping a Gaussian laser beam to a flat-top beam. Simulation results indicate that a single-zone binary phase plate can achieve excellent flat-top beam shaping quality similar to that achieved by using multiple zones. The degradation of flat-top beam shaping quality due to etching depth errors, deviation of illuminating wavelength from design value, and variation of input beam size can be compensated to some extent through on-axis adjustment of the flat-top beam observation plane. Experiments verify these theoretical expectations. The increased beam shaper fabrication tolerance can be greatly beneficial for low-cost prototyping and production of flat-top beam shapers. [DOI: 10.1117/1.1617310]

Subject terms: beam shaping; binary phase element; diffractive optics; flat top.

Paper LBS104 received Mar. 31, 2003; revised manuscript received Jul. 12, 2003; accepted for publication Aug. 1, 2003.

1 Introduction

Flat-top laser beams with uniform beam intensity distribution at the center and a sharp beam edge are useful for optical image processing, laser welding, laser radar, laser microfabrication, laser scanning, optical storage, and optical metrology. Flat-top laser beams can be realized by converting a Gaussian beam from a single transverse mode laser using an optical beam shaper. Several approaches have been reported for the design of flat-top beam shaping devices. The most straightforward method is to truncate or attenuate the input Gaussian beam using a neutral density filter with a proper transversal transmittance profile. The drawback of this approach is its poor energy efficiency. To improve the beam shaping efficiency, both reflective and refractive optical systems have been considered,[1] resulting in the requirement of sophisticated optical surfaces that are difficult to fabricate and high beam shaper fabrication costs.

Diffractive optical elements,[2] including computer-generated holograms, diffractive grating, and multilevel or quasicontinuous phase plates, show promise for highly energy efficient beam shaping applications. Geometrical transformation,[3] phase retrieval (i.e., the Gerchberg-Saxton algorithm[4] and its modified versions[5]), and simulated annealing[6,7] are main algorithms for the deign of diffractive optical beam shapers. By using these algorithms, the theoretical performance of the designed elements is excellent with a mean-square error as low as 5% and light efficiency better than 95%.[8–11] The resulting phase values range from 0 to 2π continuously in the plane of the diffractive optical element. The quality of the fabricated beam shaper depends on the accuracy of the etched surface profile and is very sensitive to etching errors. It is desired that the etched surface profile match exactly the design phase pattern requirement. The realization of such a diffractive optical element can use photolithography, electron-beam lithography, and directly laser-beam writing on photoresist or on high-energy beam sensitive glass, followed by subsequent surface profile etching. In general, accurate continuous surface profile etching[12] is hard to achieve, leading to performance degradation of the fabricated flat-top beam shapers.

Using simplified binary phase steps can greatly increase the beam shaper fabrication tolerance for low-cost flat-top beam shaper prototyping and production. Cordingley developed a single-zone binary phase plate to convert an incident Gaussian beam to a flat-top beam.[13] Veldkamp and Kastner presented the design of beam shapers using binary diffraction gratings.[14,15] Their results show that flat-top beam shapers can indeed be achieved by using a binary phase plate.

We report using a single binary phase zone to achieve efficient flat-top beam shaping with quality comparable to multizone devices. Our design simulation indicates that the degradation of flat-top beam shaping quality due to etching depth errors, deviation of illuminating wavelength from design value, and variation of input beam size can be compensated to some extent through on-axis adjustment of the flat-top beam observation plane. The experimental results have verified the theoretical expectations. The flexibility of the observation plane greatly increases the fabrication tolerance of the flat-top beam shaper, making it possible for low-cost prototyping and production.

2 Principle of Binary Phase Plate for Beam Shaping

It is well known that the Fourier transform of 1-D $\mathrm{sinc}(x)$ or 2-D $\mathrm{Bessinc}(r)$ will generate flat-top distribution, as shown in Fig. 1. The objective of flat-top beam shaping is to modulate the incident Gaussian beam profile with a proper phase function to obtain a complex field distribution as close as possible to a $\mathrm{sinc}(x)$ or $\mathrm{Bessinc}(r)$ profile, so that the distribution of the far-field laser beam at the focal

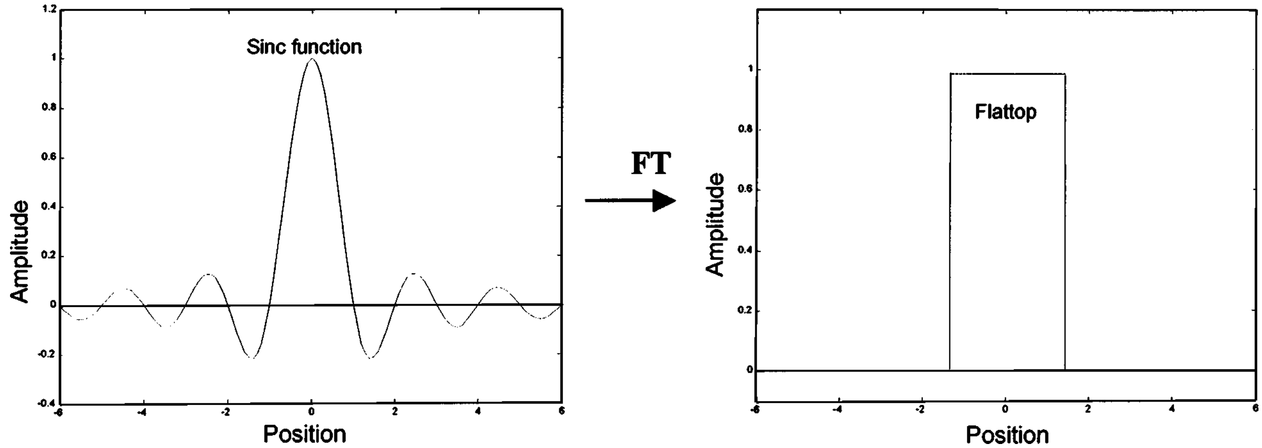

Fig. 1 Fourier transform (FT) of 1-D sinc(x) or 2-D Bessinc(r) to a flat-top output.

plane of a lens (located after the diffractive beam shaper phase plate) will be the desired flat-top beam. One simple method is to use a $(0,\pi)$ binary phase to obtain negative complex amplitude in the required areas of the phase plate, as shown in Fig. 2.

The structure of the transmission phase plate is shown in Fig. 3. Here, we consider a 2-D radial symmetric case. [For 1-D flat-top beam shaping, the Bessinc(r) function becomes sinc(x).] Here, r_0 is the zone feature size, the zone period is $2r_0$, and h is the etching depth, which results in a phase delay $2\pi(n-1)h/\lambda$ for the propagating beam of wavelength λ. We assume that the input Gaussian beam has waist radius ω_1 at $1/e^2$ peak intensity. After modulating by this phase plate, the light field is transformed by a lens with focal length f. The desired flat-top intensity distribution will be generated at the lens focal plane. The effect of the incident beam size, etching error, and wavelength deviation to the flat-top beam shaping quality is analyzed next.

3 Simulations for Analysis and Optimization of Binary Phase Plate

The input Gaussian beam amplitude can be written as

$$u_1(r_1)=\exp(-r_1^2/\omega_1^2), \tag{1}$$

with r_1 as the radial distance to the beam center. The concentric binary phase zones, as shown in Fig. 3, are represented by

$$\varphi_1(r_1)=\frac{2\pi}{\lambda}(n-1)h(r_1), \tag{2}$$

where $h(r_1)$ is the etched profile height distribution function and n is the refractive index of the phase plate at laser wavelength λ. By using a Fresnel diffraction integral, the complex light field at distance d behind the transform lens is

$$u_2(r_2)=\int_{r_1}\left\{\frac{2\pi}{j\lambda d}\exp\left(\frac{j2\pi d}{\lambda}\right)\exp\left[j\,\frac{\pi(r_1^2+r_2^2)}{\lambda d}\right]\times J_0\left(\frac{2\pi r_1 r_2}{\lambda d}\right)r_1\exp\left[-\frac{r_1^2}{\omega_1^2}+j\varphi_1(r_1)\right]\right\}dr_1, \tag{3}$$

where r_2 is the radial distance to the shaped beam center at the observation plane.

This Fresnel diffraction integral equation was evaluated by the numerical technique according to the Whittaker-Shannon sampling theorem, which is extensively applied in diffractive element design.[5,16,17] On locating the optimum observation plane, the flat-top quality is evaluated by beam uniformity, steepness, and efficiency as follows:

Uniformity:

$$U=\frac{I_{\max}-I_{\text{min valley}}}{I_{\max}}$$

in the flat-top region where intensity $>90\%$ of the peak.

Steepness:

$$K=\frac{r_2@90\%\ \text{of peak intenscity}}{r_2@10\%\ \text{of peak intensity}}.$$

Light efficiency:

$$\eta=\frac{\text{power (in region} >90\%\ \text{of peak intensity)}}{\text{total beam power}}.$$

The desired etching depth h, based on the binary phase assumption, results in a phase π in Eq. (2). This in fact depends on the zone feature size r_0 as compared to the incident Gaussian beam waist size ω_1. To let the size of the shaped flat-top beam field equal the $1/e$ width of the unshaped beam distribution in far field, we set $r_0=\omega_1$ in the design. Under this condition, we found that the optimum phase depth is not π. Figure 4 shows our calculated flat-top beam distributions under phase depths of 0.785π, 0.7925π, and 0.8π. The optimum phase depth is found to be

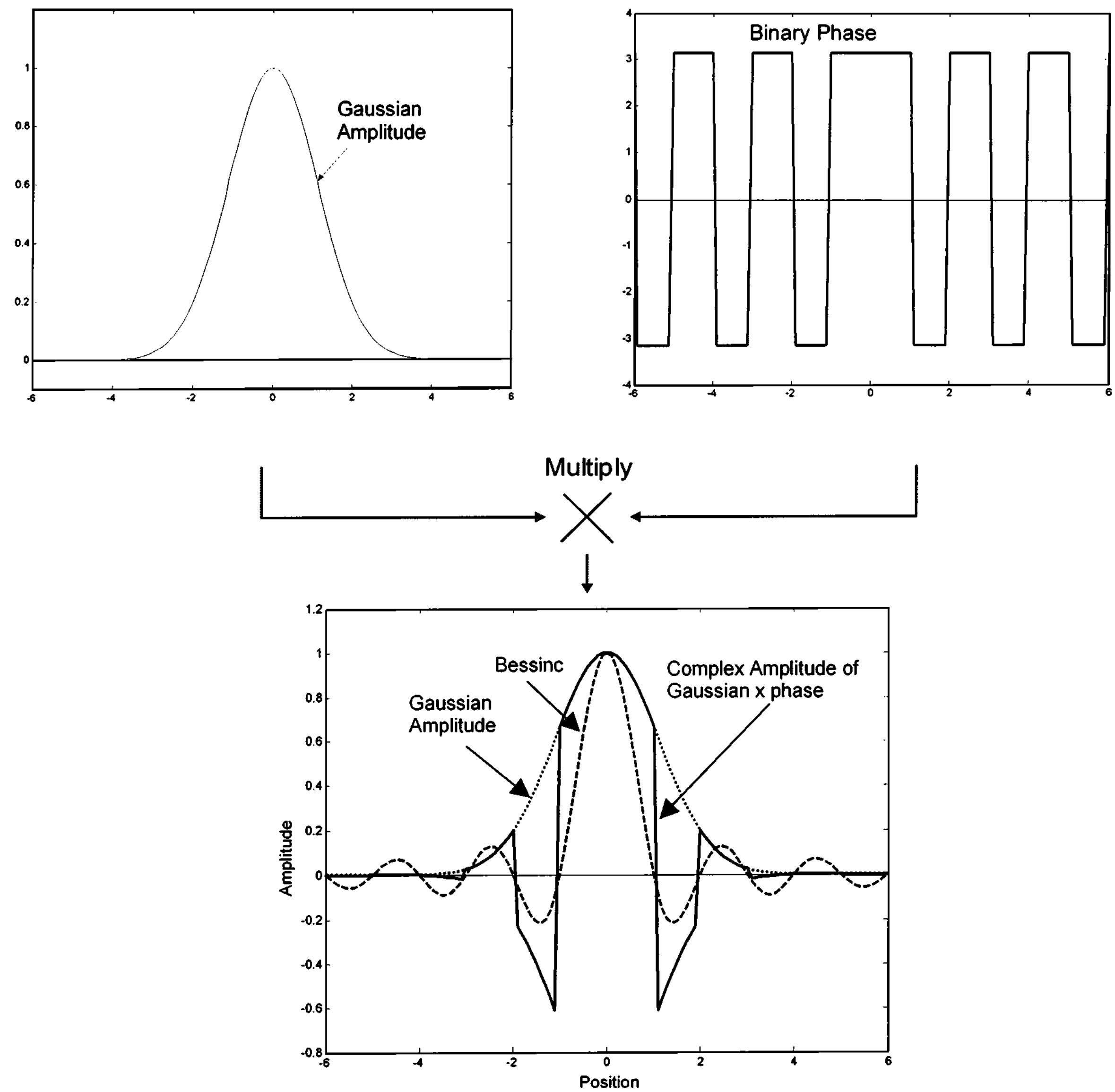

Fig. 2 Input Gaussian beam amplitude is modulated by concentric binary phase zones to generate an approximate Bessinc(r) complex field output in a radial symmetric case.

0.7925π. Under such optimum phase depth, the theoretical flat-top beam uniformity is 2.2%, the steepness is about 0.61, and the light efficiency is about 75%. For the calculations, we used an optical system with focal length $f = 400$ mm, laser wavelength $\lambda = 633$ nm, and incident Gaussian beam waist radius $\omega_1 = 420\,\mu$m. We set $d = f$. The flat-top intensity profile is shown in Fig. 5. Since wavefront property of the flat-top beam is very important,

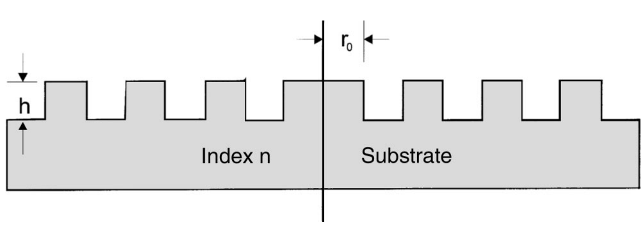

Fig. 3 Schematic of radial symmetric phase plate.

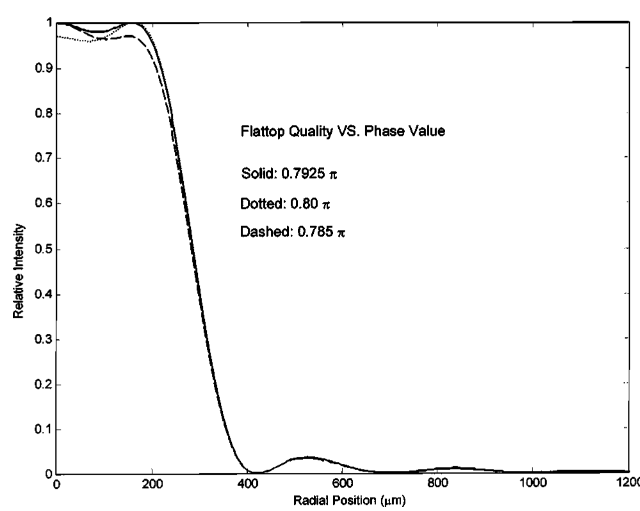

Fig. 4 Comparing flat-top beam quality under different etched phase depths, the optimal phase depth is found to be 0.7925π.

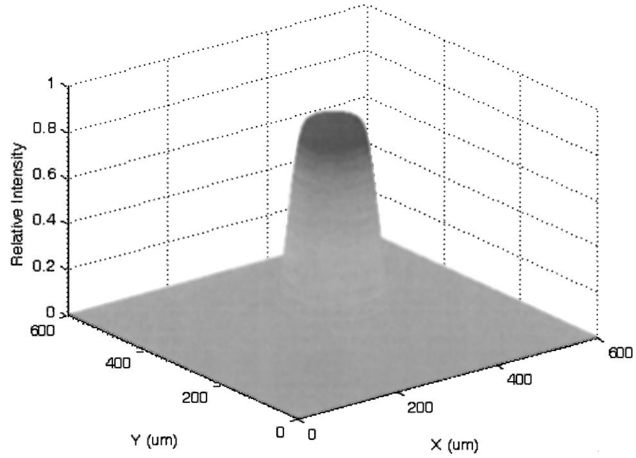

Fig. 5 Flat-top intensity profile of beam shaper with optimum phase depth.

especially in laser optics, we calculated the flat-top beam phase distribution, as shown in Fig. 6, using an optimum etching depth of 0.7925π. It demonstrates that the flat-top beam phase is relatively smooth. This is easy to understand, because the relation between the two phase distributions of the flat top and beam shaper is a Fourier transform plus a quadratic phase factor,[18] while this beam shaper has a simple phase distribution. This is also advantageous compared to those design methods based on phase retrieval algorithms,[5,16] in which the phase distributions of the beam shapers are very complicated, as are the flat-top phases. It is easy to design another phase element to correct the current flat-top beam phase into a flat phase, if necessary. In this work, we found that all of the cases discussed later have similar flat-top wavefront properties.

On the other hand, if we set the etching phase depth to be π while keeping $r_0 = \omega_1$ unchanged, we found that the best flat-top beam is not located at the focal plane of the lens. Instead it is located at $d = 0.81f$. Figure 7 shows the comparison of the shaped beam profile at different locations from the lens.

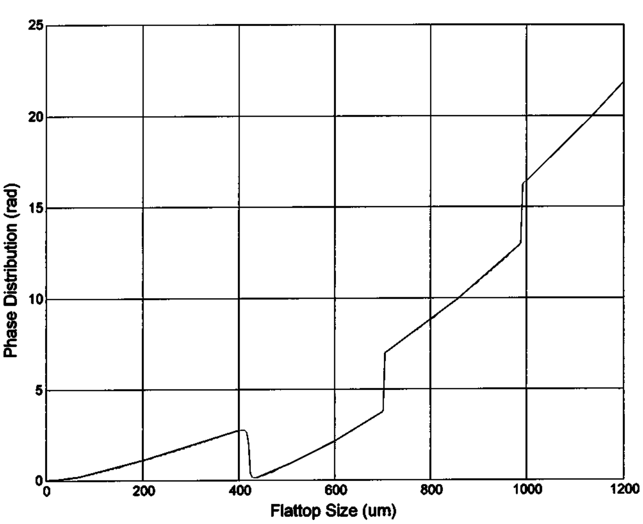

Fig. 6 Wavefront phase distribution of beam shaper with optimum phase depth.

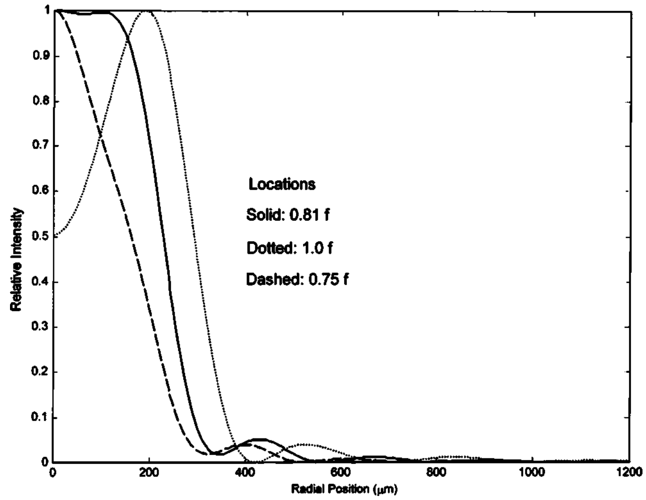

Fig. 7 Comparison of shaped beam profile at different location's from the lens when the etched phase depth is π. The best flat-top beam is located at $0.81f$.

As illustrated in Fig. 2, the flat-top beam quality will be better when using many phase zones. Using many phase zones means a larger phase area needs to be fabricated. This results in higher fabrication costs and is more time consuming for zone pattern preparation when using laser or *e*-beam writing techniques. The comparison of flat-top beam quality with different numbers of phase zones is shown in Fig. 8. By simulations, for single center zone beam shapers, we have $K = 0.5827$ and $\eta = 73.1\%$. For two-zone beam shapers, $K = 0.6136$ and $\eta = 75.35\%$. For three-zone beam shapers, $K = 0.6149$ and $\eta = 75.38\%$. We found that when the zone number is larger than 2, the flat-top quality has little improvement. In other words, the contribution of higher-order side lobes in Fig. 2 is minimal to the flat-top shaped beam quality. Thus, for practical applications, the beam shaper with two phase zones is considered enough. It can be proved that positive phase zones with

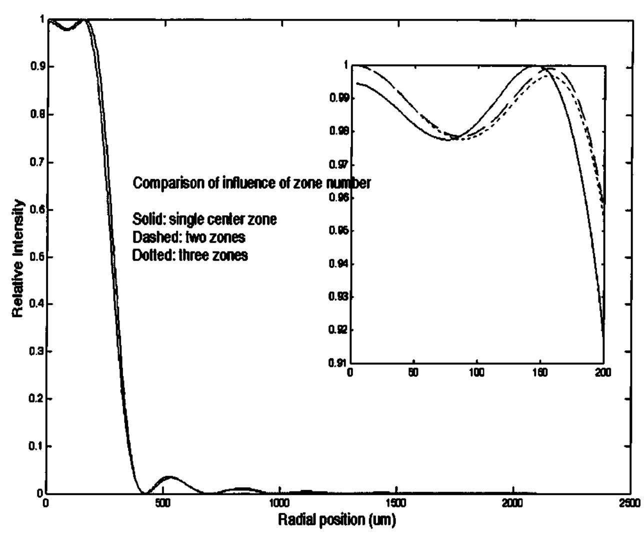

Fig. 8 Comparison of flat-top shaped beam quality as a function of etched zone number. There is no significant improvement when the binary phase zone number is larger than 2.

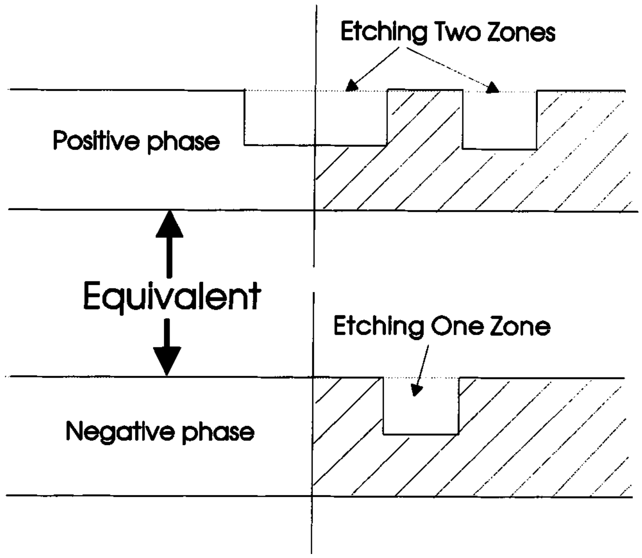

Fig. 9 For flat-top beam shaping, etching two positive ring phase zones is equivalent to that of a single negative ring phase zone.

etching at 0 to r_0 and $2r_0$ to $3r_0$ (with $r_0 = \omega_1$), as shown in Fig. 9, are equivalent to a single negative phase zone with etching at r_0 to $2r_0$ for flat-top beam shaping.[19] This way, we can just etch a single ring zone at r_0 to $2r_0$ instead of etching two ring zones. The area that needs to be etched is reduced to half. This greatly saves ring pattern preparation time if we consider laser writing or *e*-beam writing techniques. Using the single negative ring zone can achieve the same flat-top beam shaping quality as the positive two-zone beam shaper mentioned before.

The beam shaping phase plate is designed for a specific Gaussian laser waist radius ω_1. In practical applications, the flat-top shaped beam quality will be degraded when the incident beam waist radius is deviating from the design value. Consider the precise etching phase depth of 0.7925π. Increasing and decreasing the incident beam waist size by 5% of the design value results in degradation of the flat-top shaped beam quality, as shown as solid curves in Figs. 10(a) and 10(b), respectively. Such shaped beam quality degradation can be compensated by shifting the flat-top beam observation plane to $d = 0.995f$ in Fig. 10(a) and $d = 1.01f$ in Fig. 10(b). The quality compensation can also be done by a slight zoom adjustment of the lens focal length.

The accuracy of the etching depth has a great impact on the flat-top beam shaping quality. Practical surface etching may not meet exactly the phase depth requirement. The effects of 10% overetching and underetching are shown as solid curves in Figs. 11(a) and 11(b), respectively. The flat-top beam quality degradation is significant due to such etching errors. However, our calculations show that the flat-top beam shaper with such large etching errors may still be useful if we allow the flat-top beam observation plane to be shifted from the focal plane for quality compensation. Figure 11(c) shows the position of an optimal flat-top observation plane as a function of etching errors. For 10% overetching, the observation plane should be shifted to $0.92f$, as shown in Fig. 11(a). For 10% underetching, the observation plane should be shifted to $1.08f$, as shown in Fig. 11(b). The compensated flat-top beam quality is excellent.

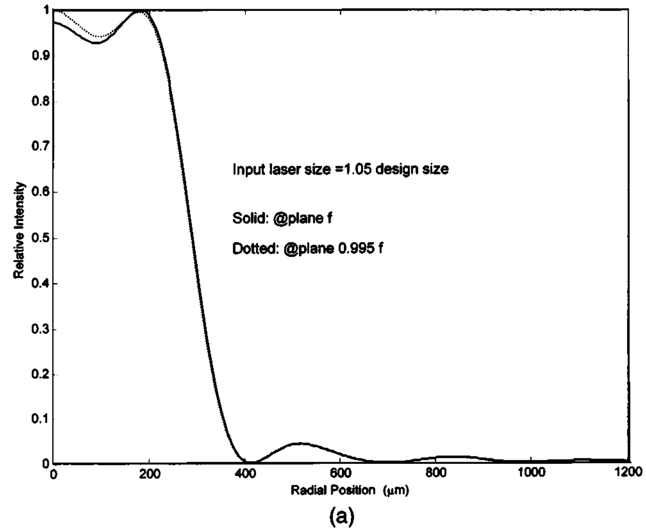

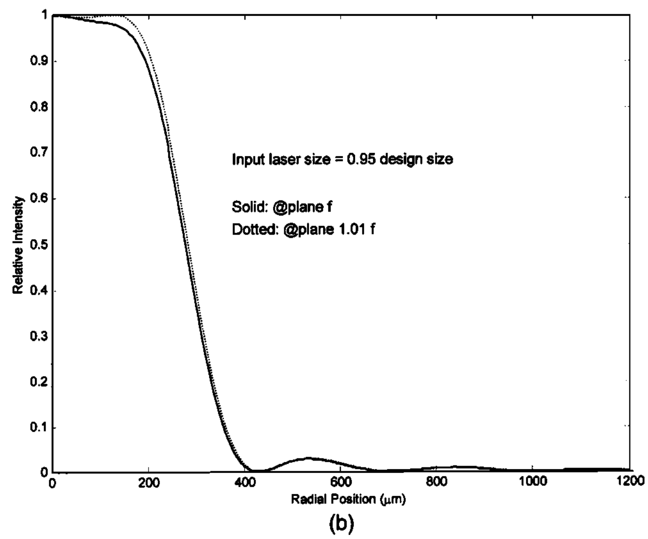

Fig. 10 Flat-top beam quality degradation when the incident laser waist size is (a) 5% larger and (b) 5% smaller than the design value (see solid curves). The quality degradation can be compensated by moving the observation plane in (a) to $0.995f$ and in (b) to $1.01f$ instead of at the focal plane.

As expected, the flat-top beam shaper is seriously constrained by the working wavelength. When the working wavelength deviates from the design value, the flat-top beam shaping quality is degraded. The sensitivity of flat-top beam shaping to the laser wavelength has been examined and we found it possible to compensate through observation plane adjustment. The position of an optimal flat-top observation plane as a function of working wavelength is shown in Fig. 12(a). Figure 12(b) gives an example where the design laser wavelength is 633 nm and the focal length is 400 mm. When the laser wavelength is changed to 570 nm, the observation plane should be at $0.925f$. When the laser wavelength is 700 nm, the observation plane should be at $1.09f$. Thus, as long as the observation plane

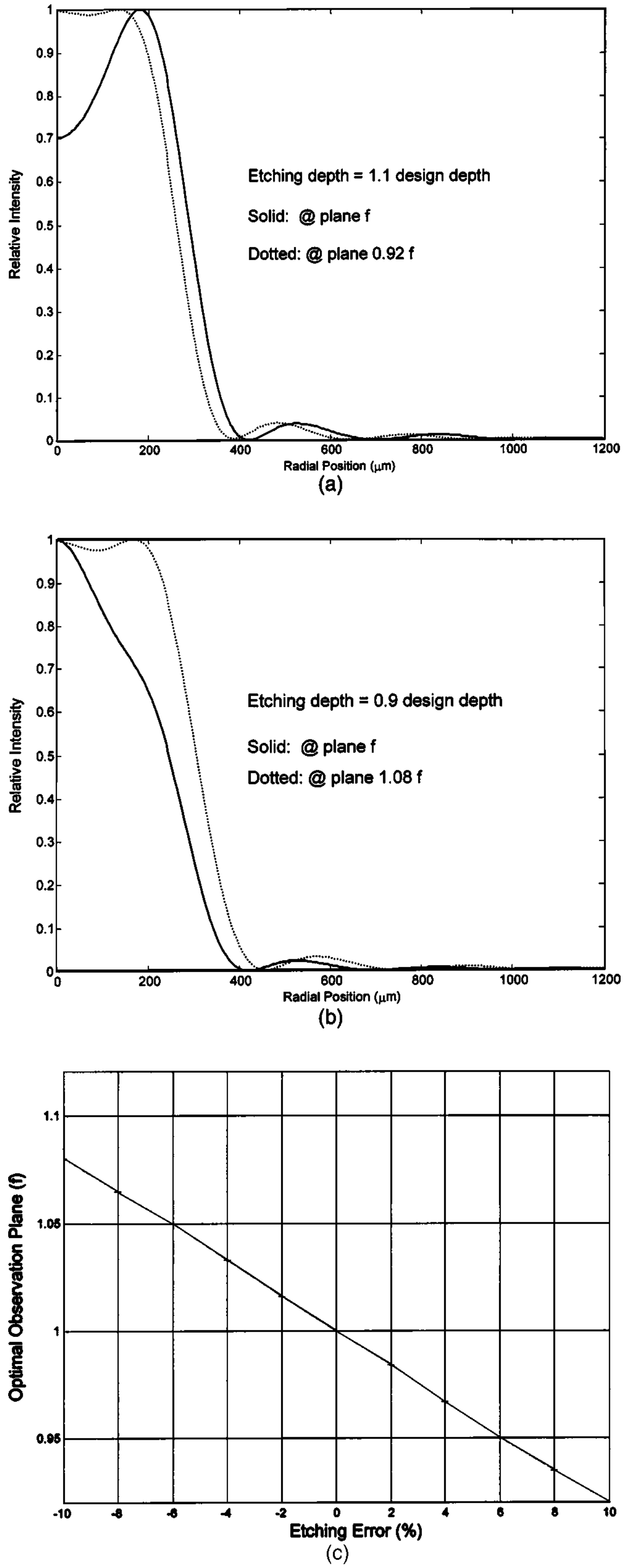

Fig. 11 There are significant flat-top beam quality degradations when the beam shaper is (a) 10% overetched and (b) 10% underetched. The flat-top quality can be compensated by moving the observation plane to 0.92f in (a) and 1.08f in (b). (c) The position of the optimal flat-top observation plane as a function of etching error.

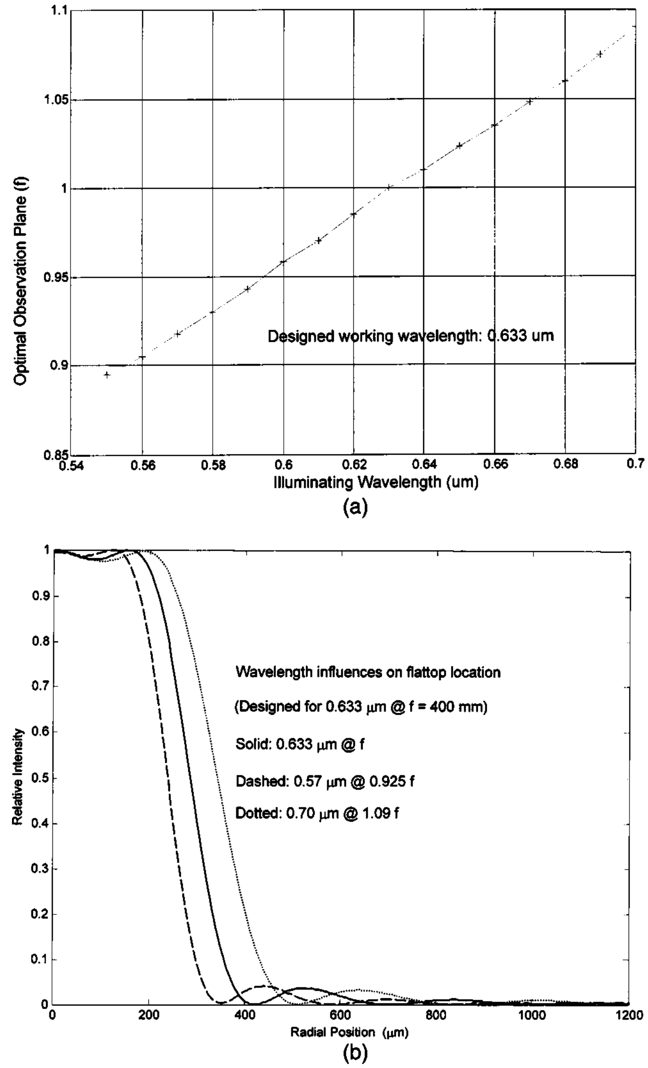

Fig. 12 A moving observation plane can compensate flat-top beam quality degradation due to the working-wavelength deviation from the design value. (a) The position of the optimal flat-top observation plane as a function of working wavelength. (b) An example for compensation of working-wavelength change.

location is not critically set, the flat-top beam shaper has a very wide working wavelength band. The flat-top beam size is, however, working-wavelength dependent, as illustrated in Fig. 12(b).

4 Experimental Results

The concept of flat-top beam shaping using a binary phase plate is examined experimentally. The schematic of the experimental setup is shown in Fig. 13, where input laser

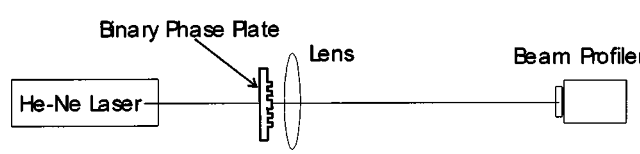

Fig. 13 Schematic of the experimental setup for measuring flat-top beam performance.

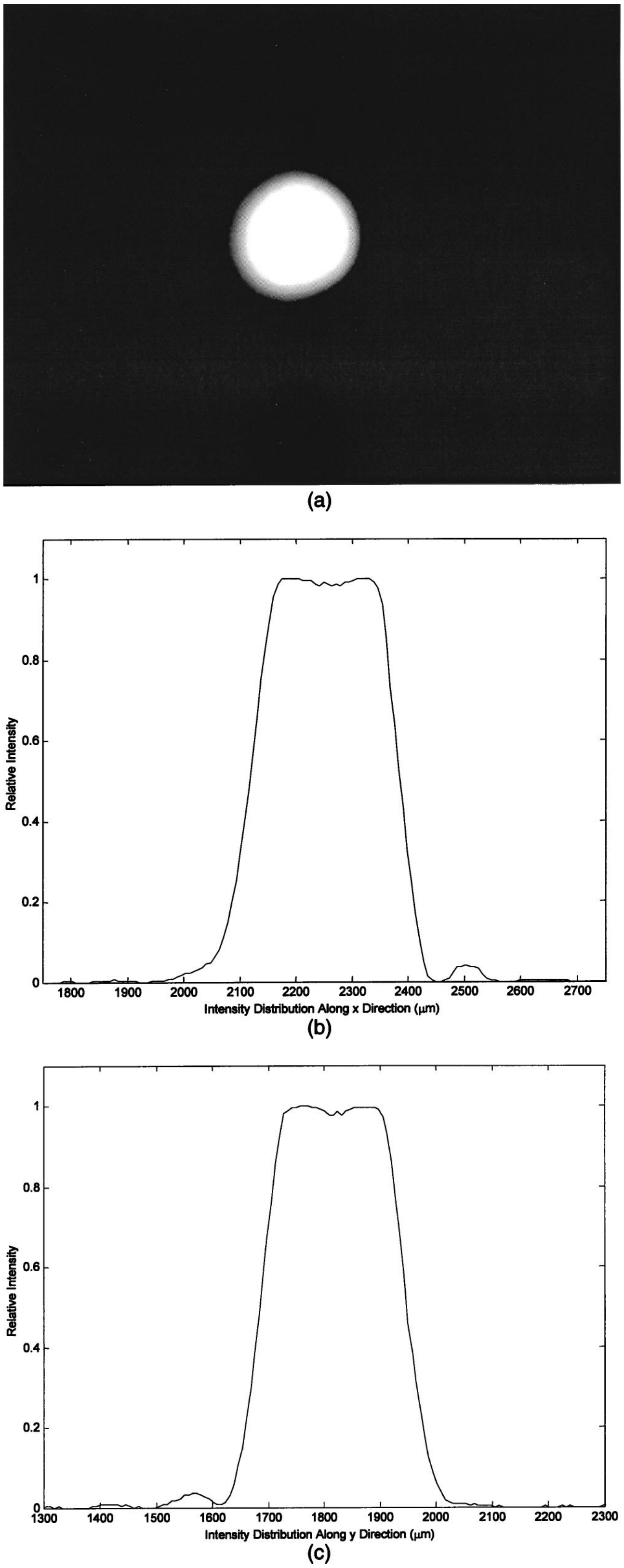

Fig. 14 Measured flat-top beam achieved by using an etched single ring zone binary phase plate. (a) Flat-top image, (b) measured beam intensity distribution in the *x* direction, and (c) measured beam intensity distribution in the *y* direction.

wavelength λ is 633 nm, Gaussian waist radius ω_1 is 420 μm, and the lens focal length f is 200 mm.

The binary phase plate is fabricated by a technique of laser direct writing on high-energy beam sensitive (HEBS) glass.[20–22] This one-step alignment-free process can result in cost-effective development of the diffractive optical elements and can support a large number of phase levels for high diffraction efficiency. Laser direct writing with controlled laser intensity and moving speed generates gray-level transmittance patterns on the ion-exchanged layer of HEBS glass. Then, direct etching the gray-level glass mask using a diluted hydrofluoric acid results in the desired surface relief profile on the glass mask surface.

The refraction index of HEBS glass at 633 nm is 1.534. To achieve the required phase step of 0.7925π, the etching depth should be 0.47 μm. The incident laser Gaussian beam waist radius is measured with a laser beam profiler to be identical to the design value. Figure 14 shows the flat-top beam achieved by using a fabricated single ring zone binary phase plate with etching at r_0 to $2r_0$, where r_0 is equal to the incident Gaussian beam waist radius of 420 μm. The etching depth of the element is measured by a Tencor Alpha-Step 100, which is 0.52 μm rather than the design value of 0.47 μm. Because of such etching depth error, we have adjusted the flat-top beam observation plane to 184 mm instead of the design focal plane position of 200 mm from the lens. The performance of the realized flat-top beam is evaluated. Around the central portion of the flat-top spot, the maximum and minimum intensities are 1.00 and 0.982, respectively, along the x axis, and 1.00 and 0.978 along the y axis, which indicate that uniformity is better than 3%. The steepness values in the x and y axes are both 0.59. The light power within an area larger than 90% intensity is 72.3%. These results demonstrate that the fabricated flat-top element has good quality that is very close to the design expectation.

For comparison, we have also designed and fabricated a double-zone binary phase plate for flat-top beam shaping. The etching ring zones are located at 0 to r_0 and $2r_0$ to $3r_0$. Again, r_0 is equal to 420 μm. The etching depth is 0.52 μm prepared in the same batch as the single-zone device mentioned before. The flat-top shaped beam observed at 184 mm from the lens has quality parameters of $U<3\%$, $K=0.59$, and $\eta=73\%$. The results are very close to the theoretical expectation and are also very close to that achieved by using a single ring zone binary phase plate.

5 Conclusions

Flat-top laser beams can be achieved by using an etched single ring zone binary phase plate instead of using multiple etched ring zones. The reduced ring zone number greatly reduces the ring pattern preparation time. The use of a binary phase plate instead of continuous surface profile etching also greatly simplifies the beam shaper fabrication. Thus, a high-quality beam shaper can be produced at low cost. Our study further indicates that etching errors, deviation of the incident beam waist size to the design value, and laser wavelength variation can degrade flat-top beam shaping quality. The quality degradation, however, can be compensated by on-axis adjustment of the shaped beam observation plane. As long as the observation plane location is not critically set, any fabricated flat-top beam shaper is considered to have a large fabrication and incident beam size tolerance, and offers a large working-wavelength bandwidth. Our experimental results verify such theoretical expectations.

References

1. D. Shealy, ''Theory of geometrical methods for design of laser beam shaping systems,'' *Proc. SPIE* **4095**, 1–15 (2000).
2. H. Herzig, *Micro-Optics: Elements, Systems & Applications*, Taylor and Francis, Ltd., London (1997).
3. O. Bryngdahl, ''Geometrical transformations in optics,'' *J. Opt. Soc. Am.* **64**, 1092–1099 (1974).
4. R. Gerchburg and W. Saxton, ''A practical algorithm for determination of phase from image and diffraction plane pictures,'' *Optik (Stuttgart)* **35**, 237–246 (1972).
5. J. Fienup, ''Phase-retrieval algorithms for a complicated optical system,'' *Appl. Opt.* **32**, 1737–1746 (1993).
6. Y. Lin, T. Kessler, and G. Lawrence, ''Design of continuous surface-relief phase plates by surface-based simulated annealing to achieve control of focal-plane irradiance,'' *Opt. Lett.* **21**, 1703–1705 (1996).
7. Q. Tan, Y. Yan, G. Jin, and M. Wu, ''Large aperture continuous phase diffractive optical element to realize uniform focal spot,'' *Opt. Lasers Eng.* **35**, 165–175 (2001).
8. Y. Lin, T. Kessler, and G. Lawrence, ''Distributed phase plates for super-Gaussian focal-plane irradiance profiles,'' *Opt. Lett.* **20**, 764–766 (1995).
9. X. Deng, Y. Li, D. Fan, and Y. Qiu, ''Pure-phase plates for super-Gaussian focal-plane irradiance profile generations of extremely high order,'' *Opt. Lett.* **21**, 1963–1965 (1996).
10. J. Liu and M. Taghizadeh, ''Iterative algorithm for the design of diffractive phase elements for laser beam shaping,'' *Opt. Lett.* **27**, 1463–1465 (2002).
11. X. Tan, B. Gu, G. Yang, and B. Dong, ''Diffractive phase elements for beam shaping: A new design method,'' *Appl. Opt.* **34**, 1314–1320 (1995).
12. X. Huang, M. Wang, and C. Yu, ''High-efficiency flat-top beam shaper fabricated by a nonlithographic technique,'' *Opt. Eng.* **38**(2), 208–213 (1999).
13. J. Cordingley, ''Application of a binary diffractive optic for beam shaping in semiconductor processing by lasers,'' *Appl. Opt.* **32**, 2538–2542 (1993).
14. W. Veldkamp, ''Laser beam profile shaping with interlaced binary diffraction gratings,'' *Appl. Opt.* **21**, 3209–3212 (1982).
15. W. Veldkamp and C. Kastner, ''Beam profile shaping for laser radars that use detector arrays,'' *Appl. Opt.* **21**, 345–356 (1982).
16. G. Yang, B. Dong, B. Gu, J. Zhuang, and O. Ersoy, ''Gerchberg-Saxton and Yang-Gu algorithms for phase retrieval in a nonunitary transform system: A comparison,'' *Appl. Opt.* **33**, 209–218 (1994).
17. D. Mendlovic, Z. Zalevsky, G. Shabtay, and E. Marom, ''High-efficiency arbitary array generator,'' *Appl. Opt.* **35**, 6875–6880 (1996).
18. J. W. Goodman, *Introduction to Fourier Optics*, 2nd ed., p. 103, McGraw-Hill, New York (1996).
19. F. Dickey and S. Holswade, ''Gaussian laser beam profile shaping,'' *Opt. Eng.* **35**(11), 3285–3295 (1996).
20. W. Daschner, P. Long, R. Stein, C. Wu, and S. Lee, ''Cost-effective mass fabrication of multilevel diffractive optical elements by use of a single optical exposure with a gray-scale mask on high-energy beam-sensitive glass,'' *Appl. Opt.* **36**, 4675–4680 (1997).
21. M. Wang and H. Su, ''Multilevel diffractive microlens fabrication by one-step laser-assisted chemical etching upon high-energy-beam sensitive glass,'' *Opt. Lett.* **23**, 876–878 (1998).
22. M. Wang and H. Su, ''Laser direct-write gray-level mask and one-step etching for diffractive microlens fabrication,'' *Appl. Opt.* **37**, 7568–7576 (1998).

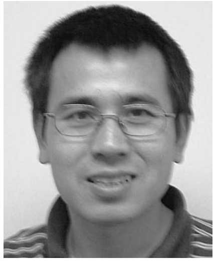

Jame J. Yang received his PhD degree in optical instrumentation in 1995 from Nankai University, China. He has been a research fellow in South Korea and Portugal, performing research in optical storage and diffractive optical element design. He has also been a research scholar at the University of Miami. He joined New Span Opto-Technology, Incorporated in 2001 as a research scientist and is currently the team leader in optics in charge of design and fabrication of optical components and optical instruments. He has been a principal investigator of several U.S. government sponsored small business innovation research and small business technology transfer projects. He has to his credit more than 30 journal publications in international journals of optics and optical engineering.

Michael R. Wang received his PhD degree in electrical and computer engineering from the University of California, Irvine. He is currently an associate professor of electrical and computer engineering at the University of Miami. Prior to joining the University of Miami in 1995, he was a team leader in photonic devices at Physical Optics Corporation, where he played a leading role in the development of integrated optical devices, wavelength division multiplexers and demultiplexers, and optical interconnect components and subsystems. His current research areas include integrated photonic devices, holographic and diffractive optical elements, optical interconnects, and optical data storages. He is the author of the article "Demultiplexing equipment" in the *Wiley Encyclopedia of Electrical and Electronics Engineering* and was a guest editor of a special issue of *IEEE Communications Magazine* on multiwavelength fiber optic communication in the December 1998 issue. He has been a principal investigator and/or project manager of more than 30 U.S. government sponsored small business innovation research, small business technology transfer, and university research programs. He has authored and coauthored more than 70 journal papers, proceedings, and conference presentations.